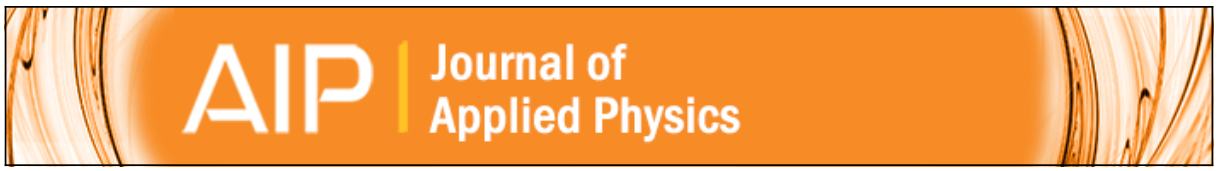


# Role of the dimensionality of the [GaX]2 network in the Zintl phases EuGa 2 X 2

Nirpendra Singh, Rainer Pöttgen, and Udo Schwingenschlögl

Citation: Journal of Applied Physics **112**, 103714 (2012); doi: 10.1063/1.4767363
View online: http://dx.doi.org/10.1063/1.4767363
View Table of Contents: http://scitation.aip.org/content/aip/journal/jap/112/10?ver=pdfcov
Published by the AIP Publishing


[This article is copyrighted as indicated in the article. Reuse of AIP content is subject to the terms at: http://scitation.aip.org/termsconditions. Downloaded to ] IP: 109.171.137.210 On: Sun, 23 Mar 2014 12:54:54

# Role of the dimensionality of the $[GaX]_2$ network in the Zintl phases $EuGa_2X_2$

Nirpendra Singh,[1,2,a)] Rainer Pöttgen,[3,b)] and Udo Schwingenschlögl[1,c)]
[1]*Physical Science & Engineering Division, KAUST, Thuwal 23955-6900, Kingdom of Saudi Arabia*
[2]*Solar and Photovoltaic Energy Research Center, KAUST, Thuwal 23955-6900, Kingdom of Saudi Arabia*
[3]*Institut für Anorganische und Analytische Chemie, Universität Münster, Corrensstraße 30, D-48149 Münster, Germany*

(Received 12 September 2012; accepted 26 October 2012; published online 28 November 2012)

The structural, electronic, magnetic, optical, and thermoelectric properties of $EuGa_2X_2$ ($X = P$, As, and Sb) are investigated using first principles calculations (taking into account the onsite Coulomb interaction) and the semi-classical Boltzmann theory. The divalent nature of Eu fulfils the Zintl principle as is confirmed by the calculated total magnetic moments of $\sim 7\,\mu_B$. A metallic behavior is obtained for all compounds. The optical spectra originate mainly from the transitions between occupied Eu 4*f* states and unoccupied Eu 5*d* states. It is demonstrated that the two-dimensional $[Ga(P/As)]_2$ network in $EuGa_2P_2$ and $EuGa_2As_2$ is favorable for thermoelectric applications as compared to the three-dimensional $[GaSb]_2$ network in $EuGa_2Sb_2$. © *2012 American Institute of Physics*. [http://dx.doi.org/10.1063/1.4767363]

## I. INTRODUCTION

Zintl phases have received great interest because of their fascinating structural variety and applications. Their physical properties include complex magnetic ordering and superconductivity.[1,2] Recently, Zintl phases have also been recognized as a new material class for thermoelectric applications.[3] Rare earth analogues of alkali or alkaline earth Zintl phases achieve the same complexity and variety as their main group counterparts but also show colossal magnetoresistance (CMR).[2] This behavior of rare earth Zintl compounds originates from interactions between the localized magnetic moments on the rare earth cations and the delocalized conduction electrons of the Zintl polyanions.

Among the rare earth Zintl phases, the Eu-containing compounds have been studied intensively.[4–8] $EuIn_2P_2$ shows a metallic behavior at room temperature.[5] Below about 60 K, it turns into a semiconductor with a very narrow energy gap, which collapses in a magnetic field of a few tesla. A strong coupling of the localized spins and the free carriers is also suggested by magneto-optical measurements.[9] The latter reveal several infrared peaks in the optical conductivity (OC) and a gain of Drude weight for growing magnetic field, which is a common feature of CMR materials. First principle calculations of the optical and magneto-optical properties of $EuGa_2P_2$ and $EuGa_2As_2$ have been reported recently.[10] The oscillator strength of the $f \rightarrow d$ transitions is found to be large at low energy, which is surprising as the probability of such transitions is very small owing to the localized character of the *f* and *d* wave functions. The Zintl compound $Eu_3Ga_2P_4$ is found to be a semiconductor with a band gap of 0.55 eV.[11] The related compound $Eu_3In_2P_4$ is reported to be a semiconductor with an energy gap of 0.42 to 0.45 eV.[5,6]

The replacement of magnetically inert cations with high moment metal cations in rare earth Zintl compounds can lead to interesting magneto-electronic properties. The magnetic properties and negative MR of $EuGa_2P_2$ and $EuGa_2As_2$ have been reported by Goforth *et al.*[12] The larger Weiss constant and higher ordering temperatures of the phosphide indicate a higher exchange energy. Recently, Schellenberg *et al.*[13] have studied the structure and magnetic properties of orthorhombic $EuGa_2Sb_2$ and found a three dimensional (3D) network between the Ga and Sb atoms which leaves large cages for the Eu atoms. This may be due to the fact that a reduced size of the pnictide converts the two-dimensional (2D) networks of $[Ga(P/As)]_2$ and $[In(P/As)]_2$ into 3D networks, as in $BaGa_2Sb_2$.[14] The interaction of the Eu atoms with the 2D $[Ga(P/As)]_2$ and 3D $[GaSb]_2$ networks can play an important role for their physical properties.

Among the compounds with a rare earth as the only magnetic element, such a large MR has only been observed for $EuB_6$[15,16] and EuO.[17–19] This stresses the importance of the investigation of rare earth Zintl phases, which bring new strategies and structural features towards useful functional materials. The structural complexity of Zintl phases makes them candidates for unusual electrical, thermal, structural, electronic, and optical properties. In this work, we investigate the Zintl compounds $EuGa_2X_2$ ($X = P$, As, and Sb) to establish the important role of the dimensionality of the $[GaX]_2$ network for the physical properties of this class of materials.

## II. COMPUTATIONAL DETAILS

The electronic structure and optical properties of $EuGa_2X_2$ ($X = P$, As, and Sb) are calculated by the WIEN2k code.[20] The generalized gradient approximation plus onsite Coulomb interaction method is used to account for the correlations of the 4*f* electrons in rare earth compounds, applying the rotationally invariant double counting scheme of Anisimov *et al.*[21] A value of $U = 7$ eV is employed as it has given a correct energy positions of the Eu 4*f* bands in previous

[a)]nirpendra.singh@kaust.edu.sa.
[b)]pottgen@uni-muenster.de.
[c)]udo.schwingenschlogl@kaust.edu.sa.

 © 2012 American Institute of Physics

[This article is copyrighted as indicated in the article. Reuse of AIP content is subject to the terms at: http://scitation.aip.org/termsconditions. Downloaded to ] IP: 109.171.137.210 On: Sun, 23 Mar 2014 12:54:54

calculations.[22] The exchange parameter $J$ is set to a usual value of 1 eV for rare earth compounds. The spin orbit interaction is incorporated via the second variational method[23] and the spin quantization axis is set along the (001) direction. The transport properties are calculated using the semiclassical Boltzmann theory[24–26] in the constant scattering approximation, as implemented in the BoltzTraP code.[27]

The calculations are performed for a mesh of 280 k-points uniformly distributed in the irreducible part of the Brillouin zone. An even finer k-mesh does not lead to any noticeable change in the eigenvalues. Self-consistency is assumed to be reached when the difference between the total energies in two successive iterations is less than 0.01 meV per atom. A dense mesh of 432 k-points is used to determine the dipole matrix elements, i.e., the optical spectra. A Lorentzian broadening of 0.1 eV is applied to simulate the effects of finite lifetime. The imaginary part of the dielectric function $\varepsilon_2$ is computed within the random phase approximation, neglecting local field and finite lifetime effects. The real part of the dielectric function $\varepsilon_1$ can be calculated from $\varepsilon_2$ using the Kramers Kronig relation. For the transport calculations, we use a mesh of 2160 k-points. As analysis tools, the band structure (BS) and density of states (DOS) will allow us to explain the optical spectra in terms of electronic interband transitions.

## III. CRYSTAL CHEMISTRY

The crystal structures of $EuGa_2P_2$[12] and $EuGa_2Sb_2$[13] are presented in Fig. 1 as views along the short unit cell axis. $EuGa_2Sb_2$ has an orthorhombic structure, while $EuGa_2P_2$ and $EuGa_2As_2$ crystallize in monoclinic structures. It is noted that the closely related Zintl compound $EuIn_2P_2$ has a hexagonal structure with space group $P6_3/mmc$.[7] The dumbbells have a single bond character with Ga-Ga distances of 241 to 249 pm in $EuGa_2P_2$ and 252 pm in $EuGa_2Sb_2$. In agreement with the divalent Eu in both pnictides, one can describe these compounds as electron precise Zintl phases $Eu^{2+}(Ga^{2+})_2(P^{3-})_2$ and $Eu^{2+}(Ga^{2+})_2(Sb^{3-})_2$. The phosphide and antimonide characters are in line with the isolated P and Sb atoms, i.e., there is no P-P and Sb-Sb bonding. Both structures are build up from $[Ga_2(P/As)_2]^{2-}$ and $[Ga_2Sb_2]^{2-}$ polyanionic networks. Nevertheless, they distinctly differ in the dimensionality of the polyanion, 2D in $EuGa_2P_2$ (and isotypic $EuGa_2As_2$[12]) and 3D in $EuGa_2Sb_2$. Small mixed occupancies observed in the structure refinements of $EuGa_2P_2$ and $EuGa_2As_2$ are not considered for the present structural description.

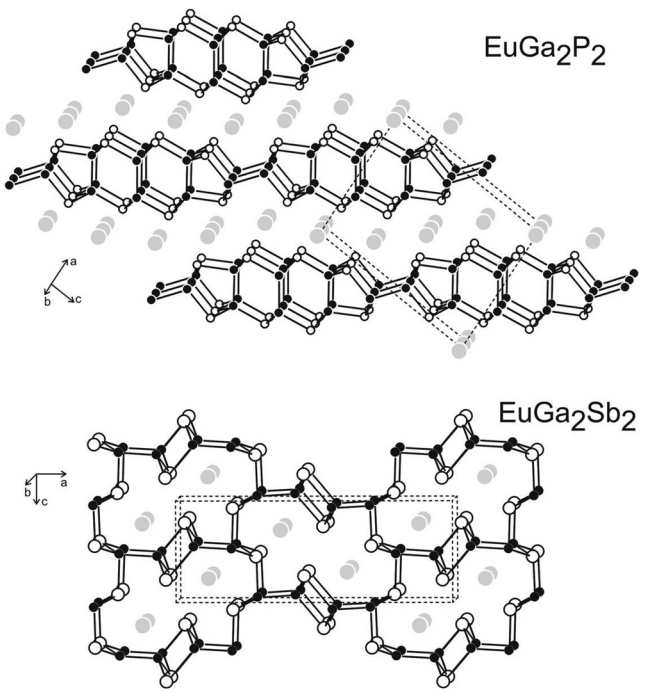


FIG. 1. Views of the $EuGa_2P_2$ and $EuGa_2Sb_2$ structures approximately along the short unit cell axis. Eu, Ga, and P (Sb) atoms are drawn as grey, black, and open circles, respectively.

The three crystallographically independent Eu atoms in $EuGa_2P_2$ as the most electropositive component have slightly distorted P coordination (294 to 312 pm Eu-P bond length). Alternatively, one can describe the $EuGa_2P_2$ structure as a stacking of anionic layers of edge-sharing $EuP_{6/3}$ octahedra that alternate with cationic layers of $Ga_2$ dumbbells. This structural principle observed for the phosphide and the arsenide is not observed for the antimonide. The arrangement of the 3D network leads to a different coordination for the Eu atoms. We also observe $EuSb_{6/3}$ octahedra. However, they are strongly distorted and the Eu-Sb distances range from 340 to 348 pm. Aside, the Eu atoms have secondary Eu-Ga contacts.

## IV. RESULTS AND DISCUSSION

After a full optimization of the experimental structure, we find small changes in the interatomic distances. We observe a Ga-Ga distances of 259.2 pm, which is slightly longer than in the experiment (252.1 pm) and in the $Ga_2$ dumb-bell of elemental Ga (244 pm). The various Ga-Sb, Eu-Sb, and Eu-Ga distances are found to be slightly changed as compared to the experiment. The Ga-Sb distances are close to the sum of the covalent radii of 266 pm, which reflects a single bond character. For the other two pnictides, we find slightly larger distances as compared to the experiment. The Eu-Eu distances in the $xz$-plane are a bit larger than those along the $y$-axis.

In order to find the magnetic ground state, we compare the total energies obtained from first principles calculations for ferromagnetic (FM) coupling and antiferromagnetic (AFM) coupling within the $xy$-plane. The calculations are carried out at the experimental lattice constants of $EuGa_2X_2$.[12,13] The calculated energy differences between FM and AFM coupling in $EuGa_2P_2$, $EuGa_2As_2$, and $EuGa_2Sb_2$ are 8.6 meV, 4 meV, and −4.8 meV, respectively. Therefore, $EuGa_2P_2$ and $EuGa_2As_2$ order ferromagnetically, while $EuGa_2Sb_2$ orders antiferromagnetically, in agreement with the experimental situation.[12,13] The calculated BSs of $EuGa_2X_2$ for the majority and minority spin states are similar to each other except for the spin minority Eu $4f$ states, which lie 9 eV above the Fermi energy ($E_F$). The calculated total magnetic moments of $EuGa_2P_2$, $EuGa_2As_2$, and $EuGa_2Sb_2$ are 6.97 $\mu_B$, 6.97 $\mu_B$, and 6.99 $\mu_B$ per Eu atom, respectively, close to the expected

[This article is copyrighted as indicated in the article. Reuse of AIP content is subject to the terms at: http://scitation.aip.org/termsconditions. Downloaded to ] IP: 109.171.137.210 On: Sun, 23 Mar 2014 12:54:54

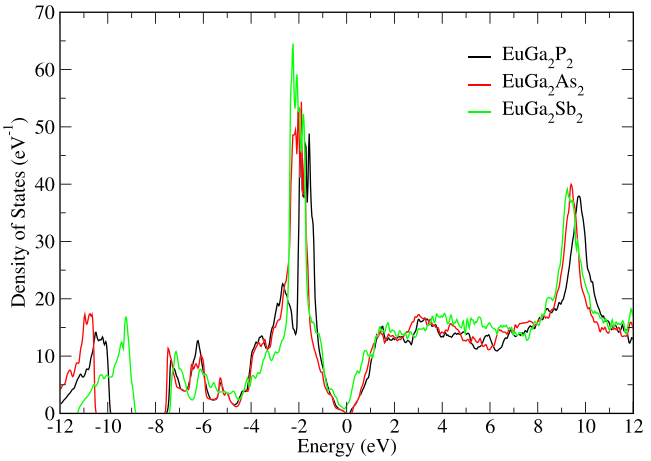


FIG. 2. Total density of states of $EuGa_2X_2$ ($X$ = P, As, and Sb).

moment for a $Eu^{+2}$ ion ($7\,\mu_B$). In that sense, the divalent nature of the Eu atoms can be readily rationalized according to the Zintl concept. By a distinct finite crossing of bands through $E_F$, the BSs characterize all three compounds under study as metals.

Corresponding total DOSs are presented in Fig. 2, reflecting the similarities already described for the BSs. While metallicity is clearly reflected by the finite DOS of $EuGa_2Sb_2$ at $E_F$, the situation is less clear for the other two compounds, but the BSs leave no doubt about their metallicity. Spin orbit interaction splits the 4*f* bands into $f_{5/2}$ and $f_{7/2}$ subbands. The spin orbit splitting is larger than the bandwidth of the subbands, which highlights the importance of spin orbit coupling in rare earth Zintl compounds. The DOS can be divided into four energy regions: Region I from −12 to −9 eV consists of the *s* states of Eu, Ga, and P/As/Sb with very small admixture of Eu and Ga *p* states. Region II from −8 to −4 eV orginates mainly from P/As/Sb *p* states with admixtures of Ga *s*, *p* and Eu *s*, *p* states. Region III from −4 eV to $E_F$ shows several sharp peaks centered at 2 eV due to the Eu 4*f* states. Finally, region IV above $E_F$ is dominated by hybridized Eu 5*d* and P/As/Sb *p*, and Ga *s*, *p* states. We note that the gross shape of the DOS shows little influence of the onsite Coulomb interaction, except for the location of the Eu 4*f* states.

The complex dielectric function $\epsilon(\omega, k)$, which describes the response of a crystal to an electromagnetic field, is calculated to further investigate the influence of the different networks. The real and imaginary components (which depend sensitively on the electronic structure of the compound) are plotted in Fig. 3 in the energy range from 0 to 8 eV, where the Drude peak is omitted for clarity. Reflecting the DOS, the dielectric functions of $EuGa_2P_2$ and $EuGa_2As_2$ are similar to each other. The zero frequency limit $\varepsilon_1(\omega \to 0)$ of $EuGa_2P_2$, $EuGa_2As_2$, and $EuGa_2Sb_2$ is found to be 16, 18, and 32, respectively. The value of $\varepsilon_1(\omega)$ is maximal at 1.7 eV, followed by a sharp decrease with energy and a deep minimum around 5 eV for $EuGa_2P_2$ and $EuGa_2As_2$ and around 3.5 eV for $EuGa_2Sb_2$. A peak at 2.4 eV and a sharp decrease thereafter are observed in $\varepsilon_2(\omega)$ for $EuGa_2Sb_2$. A similar trend is also found for the other pnictides, except that the peak is located at a significantly higher energy of about 3.5 eV. The main features of the optical spectra appear up to 5 eV. They are attributed to transitions mainly from occupied Eu 4*f* states to unoccupied Eu 5*d* states, see the DOS in Fig. 2. The anisotropy of the dielectric functions of $EuGa_2P_2$ and $EuGa_2As_2$ implies a biaxial birefringence.

The applicability of Zintl compounds as thermoelectric materials is well reported in the literature. The calculated Seebeck coefficient, electronic contribution to the thermal conductivity, and electrical conductivity of the compounds under investigation are plotted in Fig. 4 separately for the *x*, *y*, and *z*-components. For $EuGa_2Sb_2$, these components correspond to the *a*, *b*, and *c*-axis as defined in Fig. 1, respectively. On the contrary, for $EuGa_2P_2$ and $EuGa_2As_2$ only the *x* and *y*-components correspond exactly to the *a* and *b*-axis,

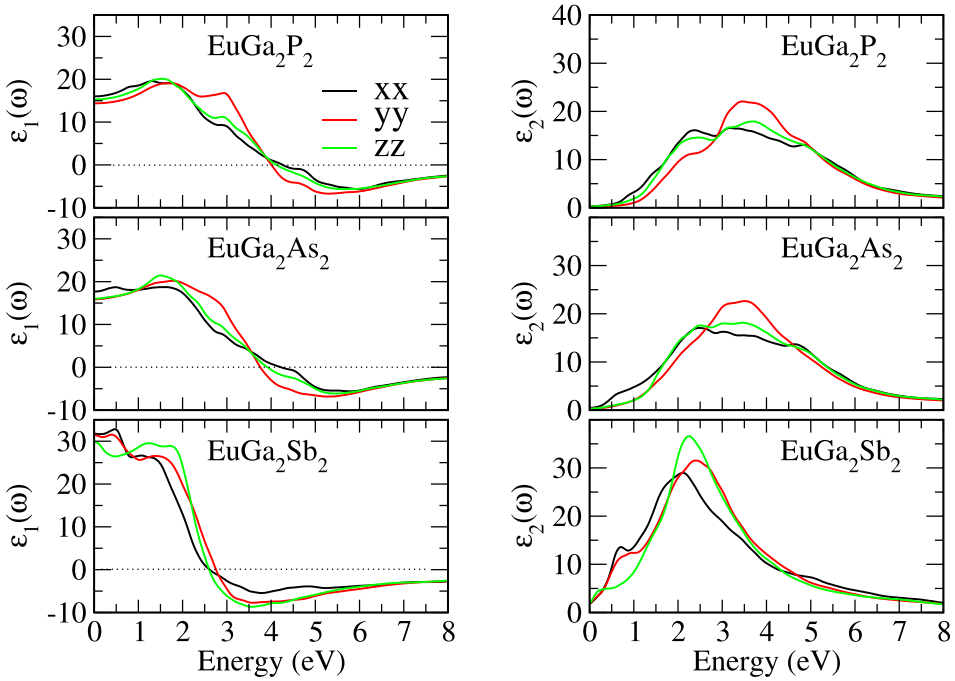


FIG. 3. Real and imaginary parts of the dielectric function of $EuGa_2X_2$ ($X$ = P, As, and Sb).

[This article is copyrighted as indicated in the article. Reuse of AIP content is subject to the terms at: http://scitation.aip.org/termsconditions. Downloaded to ] IP: 109.171.137.210 On: Sun, 23 Mar 2014 12:54:54

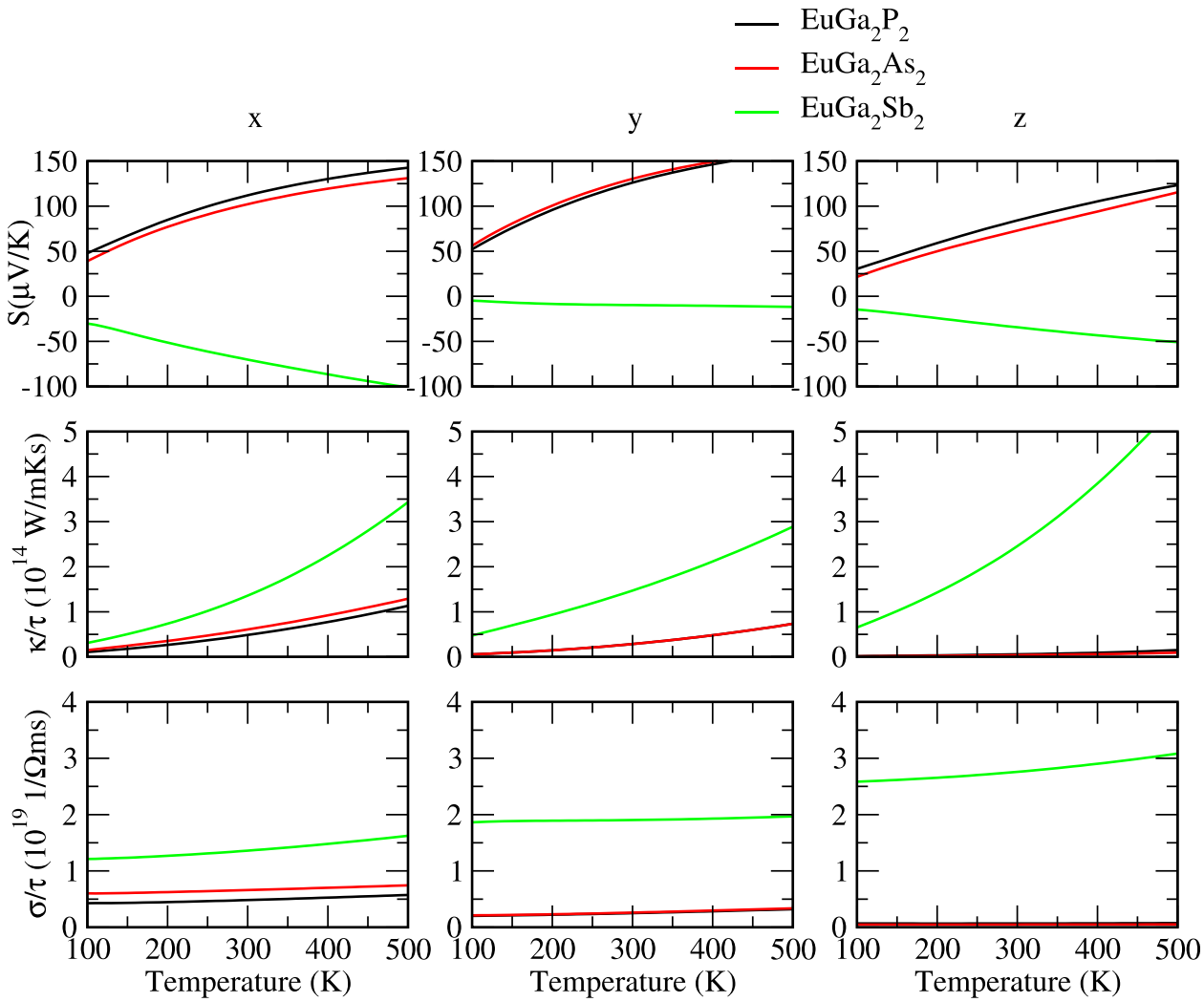


FIG. 4. Seebeck coefficient, electronic contribution to the thermal conductivity, and electrical conductivity of $EuGa_2X_2$ ($X = P$, As, and Sb).

respectively. However, because the monoclinic angles (95.5° and 95.3°) deviate not too much from 90° an approximate correspondence of the $z$-component to the $c$-axis is maintained. The Seebeck coefficient is found to be negative for $EuGa_2Sb_2$ and positive for $EuGa_2P_2$ and $EuGa_2As_2$, over the whole temperature range. This indicates that the majority carriers are electrons (n-type) in $EuGa_2Sb_2$ and holes (p-type) in $EuGa_2P_2$ and $EuGa_2As_2$. The thermopower increases with temperature with averaged values of 107 $\mu$V/K, 101 $\mu$V/K, and $-38\,\mu$V/K at 300 K for $EuGa_2P_2$, $EuGa_2As_2$, and $EuGa_2Sb_2$, respectively. The thermal conductivity increases for all three compounds with the temperature. In the case of $EuGa_2Sb_2$, it is larger by at least a factor of three and increases sharply with the temperature. The high Seebeck coefficient and low thermal and electrical conductivities of $EuGa_2P_2$ and $EuGa_2As_2$ are due to the 2D $[Ga(P/As)]_2$ network. The 2D character of the electronic structures of the phosphide and arsenide is clearly reflected by the virtually vanishing $z$-components of the conductivites, as compared to the rather isotropic transport properties of the antimonide.

To conclude, a systematic study of the Zintl phases $EuGa_2X_2$ ($X = P$, As, and Sb) is reported. Our first principles calculations reveal a metallic behavior for all compounds. We show that FM coupling is energetically favorable for $EuGa_2P_2$ and $EuGa_2As_2$, while $EuGa_2Sb_2$ favors AFM coupling. A distinctly different behavior between these two groups is also demonstrated for other electronic properties. The value of $\varepsilon_1(\omega \to 0)$ is about doubled in $EuGa_2Sb_2$ as compared to the other two pnictides. Our calculations of the optical spectra show a significant anisotropy for both $EuGa_2P_2$ and $EuGa_2As_2$, which therefore exhibit birefringence. The transport coefficients are calculated within Boltzmann theory. Larger Seebeck coefficients as well as lower thermal and electrical conductivities are found for $EuGa_2P_2$ and $EuGa_2As_2$ than for $EuGa_2Sb_2$. We conclude that the 2D network of the former compounds is favourable for thermoelectric applications as compared to the 3D network of the latter. Optical and transport measurements are highly desirable to verify the theoretical findings. Our results demonstrate that the dimensionality of the $[GaX]_2$ network establishes a major constituent for the electronic properties of rare earth Zintl phases.

## ACKNOWLEDGMENTS

R.P. acknowledges financial support by the Deutsche Forschungsgemeinschaft.

[This article is copyrighted as indicated in the article. Reuse of AIP content is subject to the terms at: http://scitation.aip.org/termsconditions. Downloaded to ] IP: 109.171.137.210 On: Sun, 23 Mar 2014 12:54:54

[1]A. M. Mills, L. Deakin, and A. Mar, Chem. Mater. **13**, 1778 (2001).
[2]J. Y. Chan, S. M. Kauzlarich, P. Klavins, R. N. Shelton, and D. J. Webb, Chem. Mater. **9**, 2131 (1997).
[3]S.-J. Kim, S. Hu, C. Uher, and M. G. Kanatzidis, Chem. Mater. **11**, 3154 (1999).
[4]A. P. Payne, M. M. Olmstead, and S. M. Kauzlarich, Chem. Mater. **13**, 1398 (2001).
[5]J. Jiang, A. C. Payne, M. M. Olmstead, H. O. Lee, P. Klavins, Z. Fisk, S. M. Kauzlarich, R. P. Hermann, F. Grandjean, and G. J. Long, Inorg. Chem. **44**, 2189 (2005).
[6]N. Singh and U. Schwingenschlögl, Chem. Phy. Lett. **508**, 29 (2011).
[7]J. Jiang and S. M. Kauzlarich, Chem. Mater. **18**, 435 (2006).
[8]A. M. Goforth, P. Klavins, J. C. Fettinger, and S. M. Kauzlarich, Inorg. Chem. **47**, 11048 (2008).
[9]F. Pfuner, L. Degiorgi, H. R. Ott, A. Bianchi, and Z. Fisk, Phys. Rev. B **77**, 024417 (2008).
[10]N. Singh and U. Schwingenschlögl, Appl. Phys. Lett. **100**, 151906 (2012).
[11]N. Tsujii, C. A. Uvarov, P. Klavins, T. Yi, and S. M. Kauzlarich, Inorg. Chem. **51**, 2860 (2012).
[12]A. M. Goforth, H. Hope, C. L. Condron, S. M. Kauzlarich, N. Jensen, P. Klavins, S. MaQuilon, and Z. Fisk, Chem. Mater. **21**, 4480 (2009).
[13]I. Schellenberg, M. Eul, and R. Pöttgen, Monatsch. Chem. **142**, 875 (2011).
[14]S. J. Kim and M. G. Kanatzidis, Inorg. Chem. **40**, 3781 (2001).
[15]C. N. Guy, S. von Molnar, J. Etourneau, and Z. Fisk, Solid State Commun. **33**, 1055 (1980).
[16]S. Sullow, I. Prasad, S. Bogdanovich, M. C. Aronson, J. L. Sarrao, and Z. Fisk, J. Appl. Phys. **87**, 5591 (2000).
[17]M. R. Oliver, J. O. Dimmock, A. L. McWhorter, and T. B. Reed, Phys. Rev. B **5**, 1078 (1972).
[18]T. Kasuya and A. Yanase, Rev. Mod. Phys. **40**, 684 (1968).
[19]A. Mauger and C. Godart, Phys. Rep. **141**, 51 (1986).
[20]P. Blaha, K. Schwarz, G. K. H. Madsen, D. Kvasnicka, and J. Luitz, *WIEN2k, An Augmented Plane Wave + Local Orbitals Program for Calculating Crystal Properties* (TU Vienna, Vienna, 2001).
[21]V. I. Anisimov, I. V. Solovyev, M. A. Korotin, M. T. Czyzyk, and G. A. Sawatzky, Phys. Rev. B **48**, 16929 (1993).
[22]J. Kunes and W. E. Pickett, Phys. Rev. B **69**, 165111 (2004).
[23]D. D. Koelling and B. N. Harmon, J. Phys. C **10**, 3107 (1977).
[24]J. M. Ziman, *Electrons and Phonons* (Oxford University Press, New York, 2001).
[25]W. Jones and N. H. March, *Theoretical Solid State Physics* (Courier Dover, New York, 1985).
[26]G. K. H. Madsen, K. Schwarz, P. Blaha, and D. J. Singh, Phys. Rev. B **68**, 125212 (2003).
[27]G. K. H. Madsen and D. J. Singh, Comput. Phys. Commun. **175**, 67 (2006).

[This article is copyrighted as indicated in the article. Reuse of AIP content is subject to the terms at: http://scitation.aip.org/termsconditions. Downloaded to ] IP: 109.171.137.210 On: Sun, 23 Mar 2014 12:54:54